Regions of convergence in a Maxwell ring-type N-body system where the central body creates a post-Newtonian potential field

Maria N. Croustalloudi[1], Demetrios Gn. Fakis[2], Tilemahos J. Kalvouridis[3]

Department of Mechanics, Faculty of Applied Sciences
National Technical University of Athens
5, Heroes of Polytechnion ave., 157 73, Athens, Greece
[1] *markr@central.ntua.gr*
[2] *e-mail: fakisdim@yahoo.gr*
[3] *e-mail: tkalvouridis@gmail.com*

Abstract. We study the regions of convergence of the equilibrium positions of a small particle in the force field of a regular polygon N body formation, where the ν=N-1 big bodies, called hereafter peripheral primaries, are located at the vertices of the fictitious regular ν-gon, have equal masses m and create Newtonian potentials, while the Nth-body (central primary) has a different mass m_0, is located at the center of the polygon and creates a post-Newtonian Manev-type potential.

1. Introduction

The N-body problem is one of the most important issues in Celestial Mechanics. In the relevant literature there are many particular cases, one of which is based upon the so-called restricted (N+1)-body regular polygon model (Scheeres, 1992; Kalvouridis, 1999; etc.), where ν=N-1 of the bodies-members of the system are spherical, homogeneous with equal masses *m*, and are located at the vertices of an imaginary regular ν-gon, while the Nth body has a different mass m_0 and is located at the center of mass of the system (Figure 1). This formation rotates around the center of mass with constant angular velocity, so that all the primaries are in relative equilibrium. A small body, natural or artificial, moves in the neighborhood of the system under the influence of all the primaries. The original version was based on the assumption that all big bodies create Newtonian force fields. Newton's theory dominated for many centuries and could explain the motion of the bodies in a very simple way. However, some physical phenomena, such as the motion of the apsidal line of the moon which was already known at that era, remained inexplicable. Newton himself knew that his theory could not give a convincing answer to this problem and for this reason inserted a corrective term in his famous formula, expressing the universal law of gravitation (Book I, Article IX, Proposition XLIV, Theorem XIV, Corollary 2 of Philosophiae Naturalis Principia Mathematica) (see

for a detailed historical review the work of Haranas-Ragos-Mioc (2011)). After Newton, many scientists tried to give a convincing answer to this problem. Some of these works appeared before the theory of Relativity, while some others appeared after it. In the latter group belong, among others, the works of Manev (1924, 1930). All these versions of the Newtonian classical potential are often referred to as post-Newtonian potentials. In 2004, Arribas and Elipe presented an improved version of the ring (N+1)-body problem. They considered that the central primary creates a post-Newtonian potential, while a little later Elipe et al. (2007) studied the periodic motions of the particle in such a dynamical system. However, in the aforementioned papers, the authors directly introduced the perturbative term in the final expression of the total potential function of the system. Here, we have reprocessed the problem from the beginning by assuming a Manev-type potential $A/r + B/r^2$ for the central primary with A=1 and B=$e\alpha$, where α is the side of the regular polygon of the configuration. The problem is characterized by three parameters, namely the number ν of the peripheral primaries, the mass parameter $\beta=m_0/m$ and the coefficient *e,* which measures the contribution of the non-Newtonian term of the potential of the central primary. Parameters ν and β are always positive, while parameter e takes small real values (<1), either positive or negative. Under these assumptions, we study the attracting regions of the equilibrium positions of the particle and we present some of the results obtained so far.

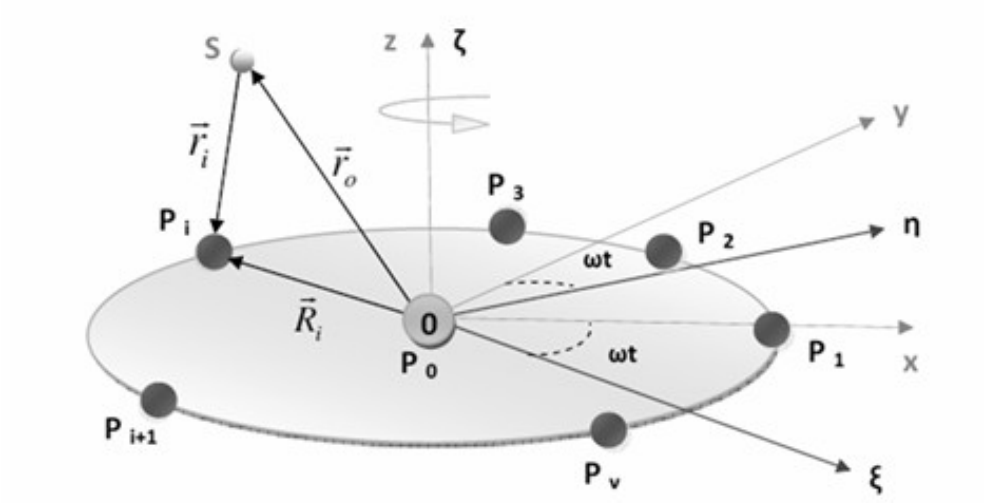

Figure 1. The configuration of the ring problem with the two coordinate systems; the inertial frame Oξηζ and the synodic one Oxyz

2. Equations of motion

We use a synodic coordinate system Oxyz centered at the central primary P_0, which is rigidly attached to the primaries. After normalization of the physical quantities,

we obtain the following dimensionless differential equations which describe the motion of the particle.

$$\begin{aligned} \ddot{x} - 2\dot{y} &= \frac{\partial U}{\partial x} = U_x \\ \ddot{y} - 2\dot{x} &= \frac{\partial U}{\partial y} = U_y \\ \ddot{z} \qquad &= \frac{\partial U}{\partial z} = U_z \end{aligned} \tag{1}$$

where

$$U(x,y,z) = \frac{1}{2}(x^2 + y^2) + \frac{1}{\Delta}\left[\beta\left(\frac{1}{r_0} + \frac{e}{r_0^2}\right) + \sum_{i=1}^{\nu}\frac{1}{r_i}\right] \tag{2}$$

is the potential function,

$$r_0 = (x^2 + y^2 + z^2)^{1/2}, \quad r_i = [(x - x_i)^2 + (y - y_i)^2 + z^2]^{1/2}$$

are the distances of the particle from the central and the peripheral primaries,

$$\Delta = M(\Lambda + \beta M^2 + 2\beta e M^3), \tag{3}$$

$$\Lambda = \sum_{i=2}^{\nu}\frac{\sin^2(\pi/\nu)}{\sin(i-1)(\pi/\nu)}, \quad \mathrm{M} = 2\sin(\pi/\nu)$$

There is a Jacobian-type integral of motion,

$$\dot{x}^2 + \dot{y}^2 + \dot{z}^2 = 2U(x,y,z) - C \tag{4}$$

3. Equilibrium points and zones - Parametric evolution- Stability

As it is known, in an equilibrium position we have the conditions

$$\dot{x} = \dot{y} = \dot{z} = \ddot{x} = \ddot{y} = \ddot{z} = 0$$

Then,

$$\begin{aligned} \frac{\partial U}{\partial x} &= U_x = 0 \\ \frac{\partial U}{\partial y} &= U_y = 0 \\ \frac{\partial U}{\partial z} &= U_z = 0 \end{aligned} \tag{5}$$

Their exact locations are calculated numerically by solving (5) using a numerical method. In the gravitational case, Kalvouridis (1998) proved that the existing equilibrium positions are all located on the plane *Oxy* of the primaries' motion and are grouped on either five or three equilibrium zones according to parameter β. If $\beta \geq l_v$ the existing equilibrium zones are three (A_1, C_2, C_1) (Figure 2a), otherwise the equilibrium zones are five (A_1, A_2, B, C_2, C_1) (Figure 2b). Each zone consists of ν equilibrium positions. Zones A_1 and A_2 evolve inside the fictitious circle of the peripheral primaries and very close to each other. Zones C_2 and C_1 evolve outside the circle of the peripheral primaries. Finally, the equilibria of zone B appear close to the circle of the primaries and between them.

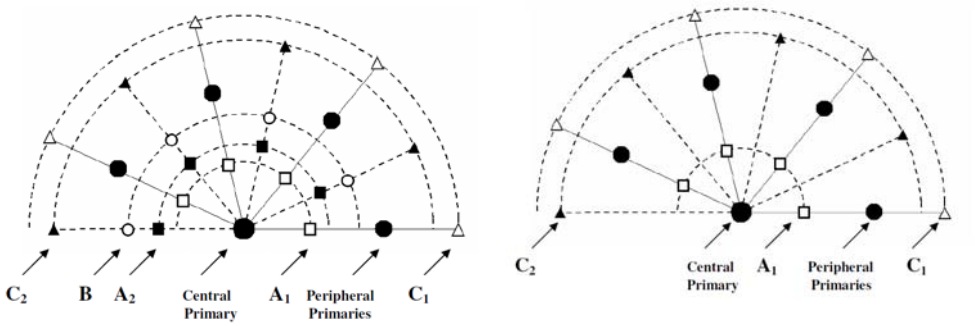

Figure 2. (a) $\beta<l_v$, five equilibrium zones, (b) $\beta \geq l_v$, three equilibrium zones. Black dots denote the positions of the primaries

In the considered case with a central body creating a Manev's potential, if $e>0$, then the equilibrium zones are either five or three as in the gravitational case. However, this transition depends on both parameters β and e. Figure 3 shows the bifurcation curve of the equilibrium zones for ν=7. In the area below the bifurcation curve (region I) there are five equilibrium zones, while above it (region 2) there are only three equilibrium zones. This curve is very well approximated by the third-order polynomial,

$$P(x) = 3.1008 - 8.02052x + 16.9227x^2 - 17.9331x^3$$

As the number ν of the peripheral primaries increases, this curve is displaced towards the upper part of the diagram. In other words, region I, extends to higher values of parameter β. Table 1 shows some indicative pairs of values (β, e), where this bifurcation occurs. Here, we note that for the considered problem where only the central primary creates a post -Newtonian potential, the symmetry of the distribution of the equilibrium points is preserved regardless of the value of parameter e.

e	ν = 7	ν = 9
	β_ν	β_ν
0.0001	3.100	8.255
0.001	3.093	8.239
0.01	3.022	8.100
0.055	2.708	7.443
0.1	2.455	6.890
0.209	2.000	5.840

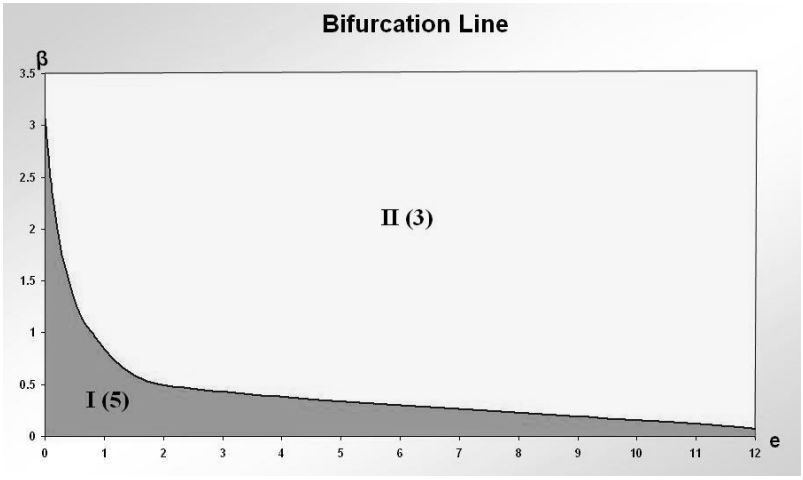

Figure 3. Bifurcation curve for ν=7. Below the curve (region I) five equilibrium zones exist, while above it (region II) the equilibrium zones are only three

If e<0, two new groups of planar equilibrium positions may appear, namely E_1 and E_2 which evolve inside the circle of the peripheral primaries and very close to the central primary. Apart from the planar equilibria and for certain combinations of values of e and β, two more out-of-plane equilibrium positions (L_{-Z} and L_{+Z}) have been found on the z-axis of the synodic system and in symmetric positions with respect to the xy-plane. The number of the planar equilibrium zones depends on both parameters β and e. Figure 4 is a bifurcation diagram showing the number of the existing equilibrium zones on the xy plane for ν=7 and for various values of e and β.

There are three bifurcation lines BL_0, BL_1 and BL_3 which intersect or converge and coincide in some parts of the diagram separating in this way the area (e,β) in five

regions. We have found that the following general rules govern the number and the type of the existing equilibrium zones in these regions:

- On the left side of BL_0, zones B and A_2 appear.
- On the left side of BL_1, zones E_1 and A_1 disappear.
- On the left side of BL_2, zones A_2 and E_2 do not exist.

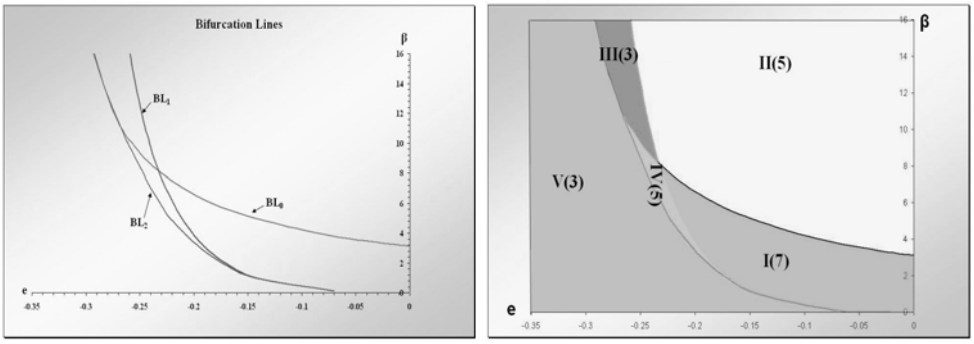

(a) (b)

Figure 4. Bifurcation diagram e-β of the equilibrium zones for ν=7 and e<0; (a) bifurcation curves BL_0, BL_1 and BL_2, (b) regions I, II, III, IV and V with the number of the existing equilibrium zones

Provided that in region II five equilibrium zones exist, namely, zones C_2, E_2, E_1, A_1, C_1, then according to these rules, in region I there are seven zones, namely, C_2, B, A_2, E_2, E_1, A_1 and C_1; in region IV five equilibrium zones exist, namely, zones C_2, B, A_2, E_2 and C_1; in region IV there are three zones, namely C_2, E_2 and C_1 and finally, in region V the existing zones are three, that is, C_2, B and C_1.

Figure 5 shows the distribution of the equilibrium points in each of the aforementioned five regions of the bifurcation diagram.

4. Procedure for the determination of the regions of convergence

As we mentioned before, the non-linear algebraic system (5) is solved numerically by using an algorithm, provided that an initial approximation is given. The iterative process stops at the desired target which is an equilibrium point. We can consider the process of the consecutive iterations as one, where the determination of successive approximating values-points forms a crooked path-line leading to the desired target, which is an equilibrium point. As a consequence, the set of the initial points that lead to the points of a particular equilibrium zone is called an “attracting domain” or “region of convergence” or “basin of attraction” (Croustalloudi and Kal-

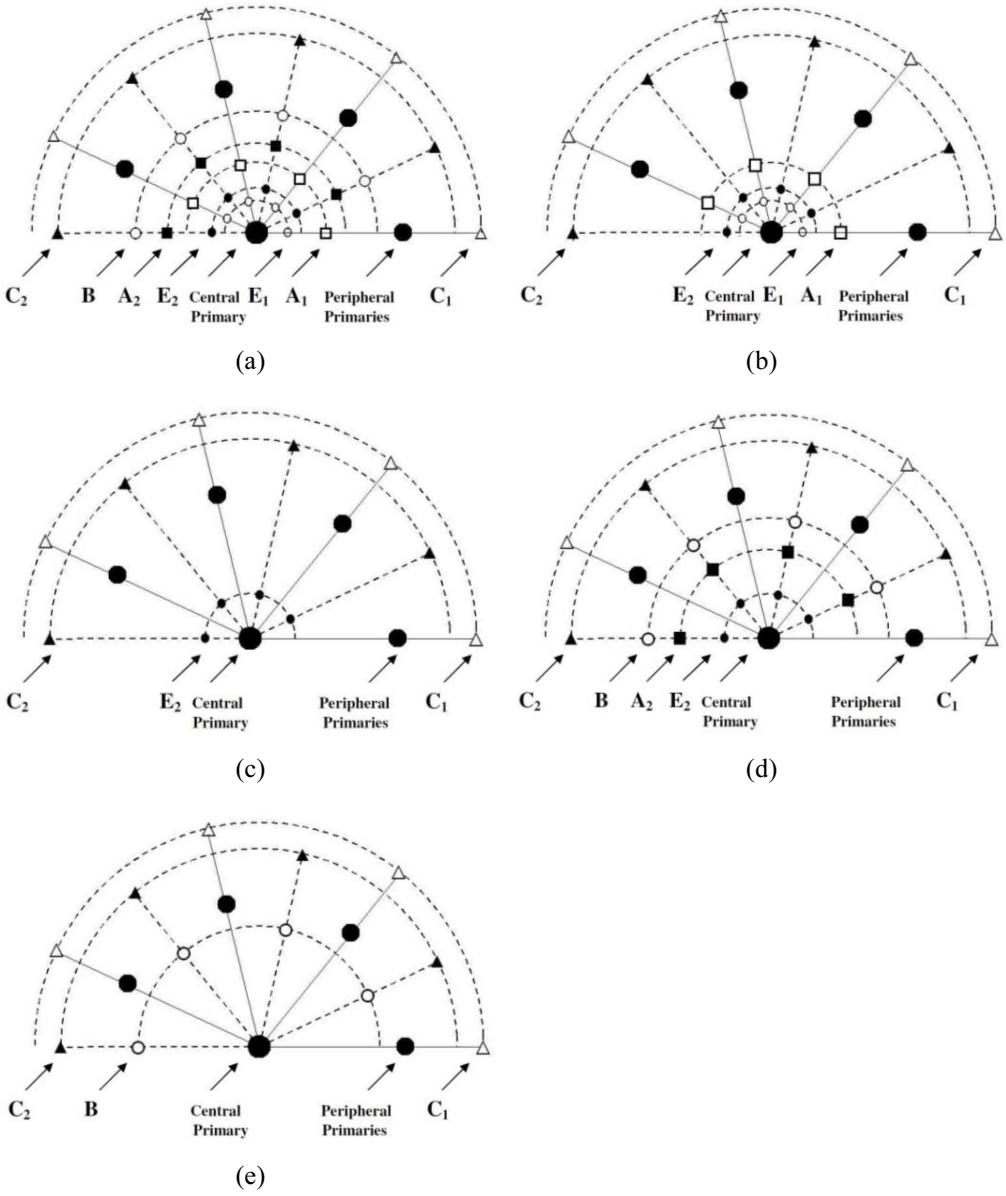

Figure 5. Distribution of the equilibrium points on the existing zones for $e<0$; (a) region I (seven zones), (b) region II (five zones), (c) region III (three zones), (d) region IV (five zones), (e) region V (three zones). Black dots are the locations of the primaries

vouridis, 2004, 2007; Kalvouridis, 2009). We shall use hereafter all three terms. We restrict our investigation to the planar equilibrium zones (z=0) and we apply the well-known Newton-Raphson's method by scanning both axes of plane Oxy in the intervals $x_o \in [-2.5,0) \cup (0,2.5]$, $y_0 \in (0,2.5]$ with steps $\Delta x_0 = \Delta y_0 = 0.005$. The converging initial pairs (x_0, y_0) are then separated in as many groups as the number of the existing equilibrium zones. At the same time, we record the number of the iterations (steps) required to find an equilibrium position with a predetermined accuracy (here 10^{-8}). The attracting domain of each zone presents, as it is expected, all the symmetry elements of the primaries' arrangement. It generally consists of some "compact" parts, that is, areas all the points of which lead to the equilibrium positions of this particular zone and therefore show a deterministic aspect since small alterations in their values lead to the same target. There are also dispersed points that lie on the boundaries of the "compact" regions of this or other zones. Therefore, these boundaries are not clearly defined and are characterized by a chaotic behavior in the sense that these points are very sensitive to small alterations of their values, so that the prediction of their final destination becomes extremely difficult.

5. Evolution of the regions of convergence of the zones when e is negative - Parametric dependence

In what follows we shall restrict our study to the case $e<0$, since the case with $e>0$ is very much alike to the gravitational one; except that the transition from five to three zones depends on both parameters e and β (see Figure 2, in section 3). An analytical description of the evolution of the attracting domains in this case can be found in a previous article by two of us (Croustalloudi and Kalvouridis, 2007). As we have mentioned in section 3, there are five different possibilities according to the combination of values of e and β. We shall proceed to describe two sample cases; the first one concerns a pair of (e,β), for which all seven equilibrium zones exist (region I of the diagram of Figure 4) and the second one concerns a pair (e,β), which falls in the region V, where only three zones, namely, C_2, B and C_1, exist.

5.1. Evolution of the regions of convergence when (e,β) falls into region I of the bifurcation diagram

There are seven equilibrium zones, namely E_1, E_2, A_1, A_2, B, C_2 and C_1 (see Figure 6a). Regarding the attracting domains of zones E_1 and E_2, we observe a dense distribution inside an almost circular area which surrounds the central primary. The compact parts of this distribution are very narrow and evolve along the directions of the radii where the equilibrium points lie. In this circular area, besides the dispersed points that belong to E_1 and E_2, we also observe points that belong to the remaining five zones. Dispersed points of these zones are also found beyond this central circular area; these form repetitive patterns with a fractal structure. Figures

6a and 6b show the evolution of these zones, while Figures 6c and 6d are magnifications of the circular areas of these zones.

The attracting domain of zone A_1 presents "compact", diamond-shaped parts with wavy and vague boundaries developing between each peripheral primary and the previously described circular area of zones E_1 and E_2. Inside these areas lie the equilibrium positions of that zone (Figure 6e). The more β augments, the more these areas expand in a way that their radial dimension remains steady, while their maximum transverse dimension increases. This expansion causes an approximation of the consecutive "compact" areas of that zone.

The "compact" regions of zone B (when it exists) develop between the consecutive peripheral primaries, whose positions lie on the contacts of these regions. Their form is similar to that of the "compact" regions of A_1, but their boundaries are more indented, sharp and vague (Figure 6g). When β increases their radial dimension is compressed, while their transverse dimension remains almost stable.

The attracting domains of zone A_2 develop between the "compact" regions of zones A_1 and B and the circular area of the dense distribution of the points of zones E_1 and E_2, thus creating a kind of three-legged formations, one part of which evolves toward the direction of the radius that connects the origin of the axes with an equilibrium position of that zone, while the other two develop toward the directions connecting the particular position with two neighboring peripheral primaries (Figure 6f). In each of these formations is observed a basic "compact" region, which surrounds the corresponding equilibrium point and is more expanded than the others. The development of the rest of the "compact" regions toward the aforementioned directions is characterized by self-similarity with shapes whose dimensions diminish as they approach a central primary or a peripheral one. The "compact" regions of A_2 are framed by dispersed points, which accumulate around them and evolve in a similar way. Contrary to what takes place in A_1, the more β augments, the attracting regions of A_2 reduce due to the drastic reduction of the dispersed points that border the "compact" regions.

The attracting area of C_1 is extremely complex and is therefore difficult to be described geometrically. We could generally say that each formation consists of two basic "compact" regions, the biggest of which contains the equilibrium point (Figure 6i). As regards the dispersed points, on the one hand they are organized in a dense way forming meniscus that surround the two basic "compact" regions, and on the other hand, they are diffused at the boundaries of the "compact" regions of the other zones.

In the plane areas that lie between the "compact" regions of zones C_1 and B stretch the "compact" regions of the attracting area of zone C_2, which have the form of a mushroom and contain the equilibrium points of this zone (Figure 6h). The dispersed points surround densely the "compact" regions, but also diffuse at the boundaries of the compact regions of the other zones. As β augments, but the pair (e,β) remains at the same region of the bifurcation diagram of Figure 3, the "com-

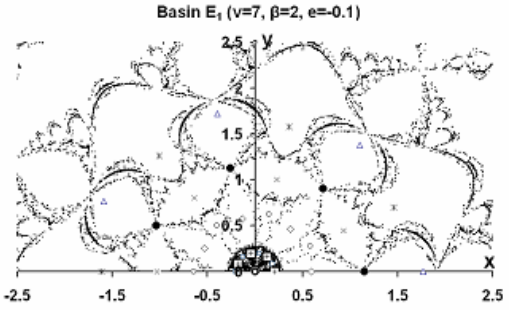
Basin E1 (ν=7, β=2, e=-0.1)
y
x
2.5
2
1.5
1
0.5
0
-2.5
-1.5
-0.5
0.5
1.5
2.5

(a)

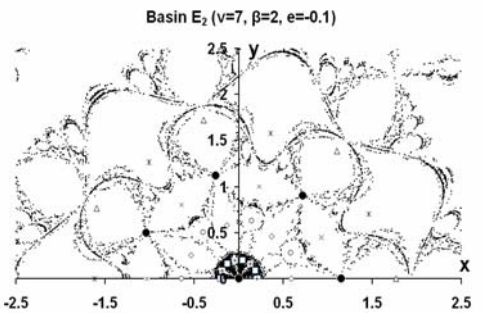
Basin E2 (ν=7, β=2, e=-0.1)
y
x
2.5
2
1.5
1
0.5
0
-2.5
-1.5
-0.5
0.5
1.5
2.5

(b)

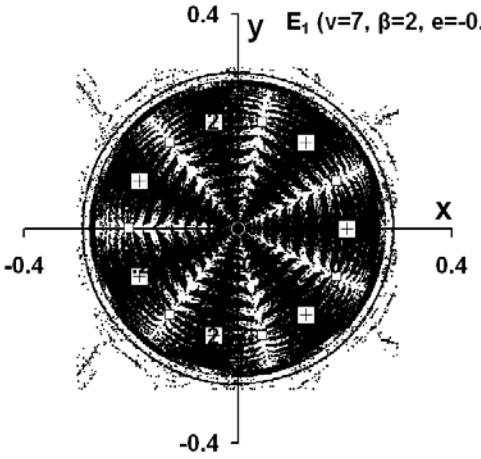
E1 (ν=7, β=2, e=-0.1)
y
x
0.4
-0.4
0.4
-0.4

(c)

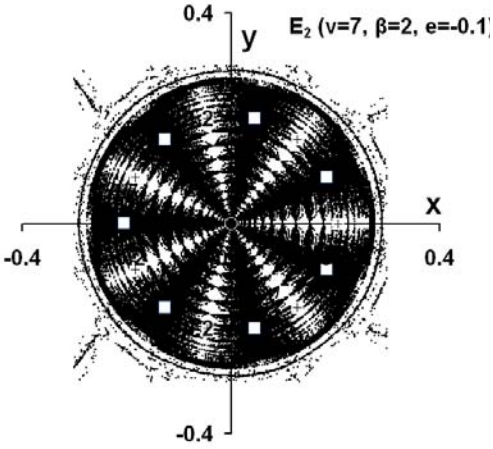
E2 (ν=7, β=2, e=-0.1)
y
x
0.4
-0.4
0.4
-0.4

(d)

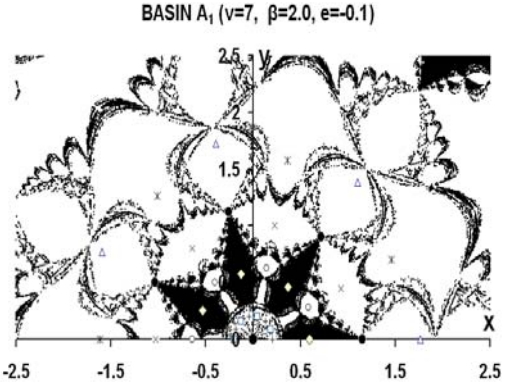
BASIN A1 (ν=7, β=2.0, e=-0.1)
y
x
2.5
2
1.5
0
-2.5
-1.5
-0.5
0.5
1.5
2.5

(e)

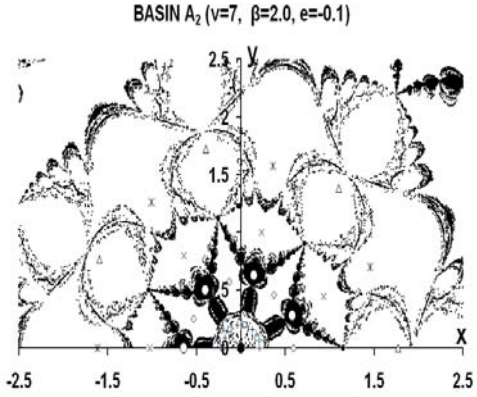
BASIN A2 (ν=7, β=2.0, e=-0.1)
y
x
2.5
2
1.5
0
-2.5
-1.5
-0.5
0.5
1.5
2.5

(f)

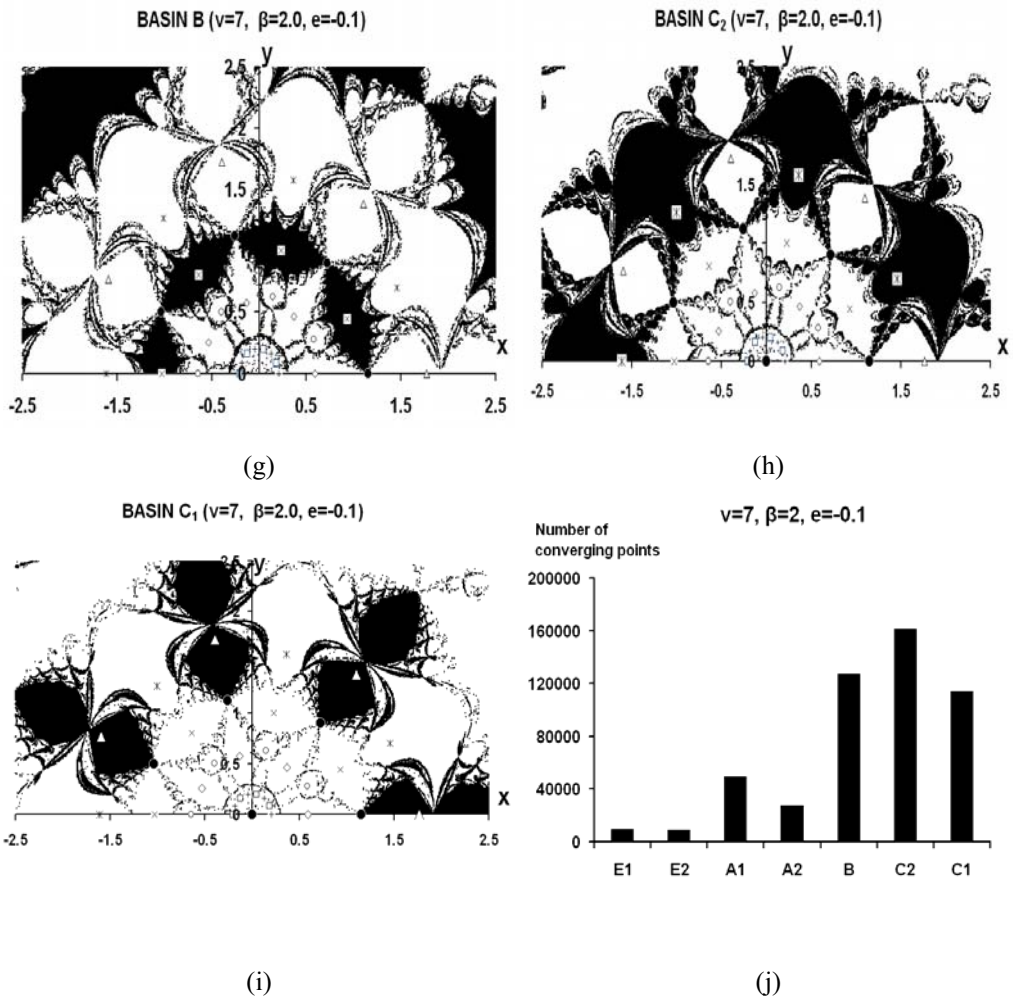

Figure 6. Attracting domains for a configuration with ν=7 and β=2, e=-0.1 (region I of the bifurcation diagram-seven equilibrium zones); (a) zone E_1, (b) zone E_2, (c)-(d) details of the central parts of zones E_1 and E_2, (e) zone A_1, (f) zone A_2, (g) zone B, (h) zone C_2, (i) zone C_1, (j) bar chart showing the number of the converging points of each equilibrium zone

pact" regions are slightly reduced, while the dispersed points get denser. Nevertheless, the total attracting domain of the zone is reduced. As a general remark, we note that at the values (e, β) which lie on the bifurcation curves, there is an abrupt change in the number and type of equilibrium zones, which results in a change (increment or decrement) of the points of the attracting domains of the existing zones.

The bar chart of Figure 6j shows the number of the converging points of each equilibrium zone. It is evident that the attracting domains of zones E_1 and E_2 are the smallest ones, while the basin of attraction of zone C_2 is the largest.

5.2. Evolution of the regions of convergence when (e,β) falls into region V of the bifurcation diagram

As a sample case we have used the set of values ν=7, β=2, e=-0.2. From the diagram of Figure 4b we see that only three equilibrium zones exist, namely, C_1, B and C_2 (see also Figure 5e). Figure 7 shows the attracting domains of these zones. The "compact" regions of these domains have the basic characteristics that were described in the previous case. However, in the area which extends between the central primary and the peripheral ones for each zone, the dispersed points are densely distributed and form a fractal-like structure which is quite similar to all three zones (Figure 7a, b, c).
The bar chart of Figure 7d shows the number of the converging points to each equilibrium zone. Evidently, the attracting domain of zone C_1 is the smallest one, while that of zone C_2 is the largest one.

6. Areas of more or less consuming computing time

Our next step was to study the way with which the attracting domain of an equilibrium zone is resolved into smaller regions, according to the number of the steps needed to reach the equilibrium positions of this particular zone. This resolution is related with the speed of convergence and, consequently, with the economy in computing time, a fact that is important for both the speed and the accuracy of computations. As we have already stressed in section 3, the number of the required steps in order to achieve the location of an equilibrium position depends on the numerical method used and on the predetermined accuracy. However, the results we obtained when we used the same method (Newton-Raphson) and a variety of values for accuracy, presented such similar images, that general results can be deduced. In order to achieve the specific goal, we considered the class intervals 1-5 (very fast convergence), 6-10 (fast convergence), 11-15 (moderate convergence), 16-20 (slow convergence) and >20 (very slow convergence) for the number of steps and accuracy of 10^{-8}. The general observations that concern all the zones can be summarized as follows:

- The subset of the "launching" points of the (x, y) plane corresponding to the class interval 1-5 steps (very fast convergence) for any equilibrium position of any equilibrium zone, consists of a "compact" region which occupies the central "compact" part of the attracting domain around each equilibrium position of this particular zone and of a few dispersed points which appear near these areas or between the "compact" regions of other zones.
- The subset of the points corresponding to the class interval 6-10 steps (fast convergence) of each zone, consists of "compact" regions which complement the "compact" regions of the class interval 1-5 steps and of a large number of isolated points of the attracting area of this particular zone. These points are spread in a widely extended area of the (x, y) plane.

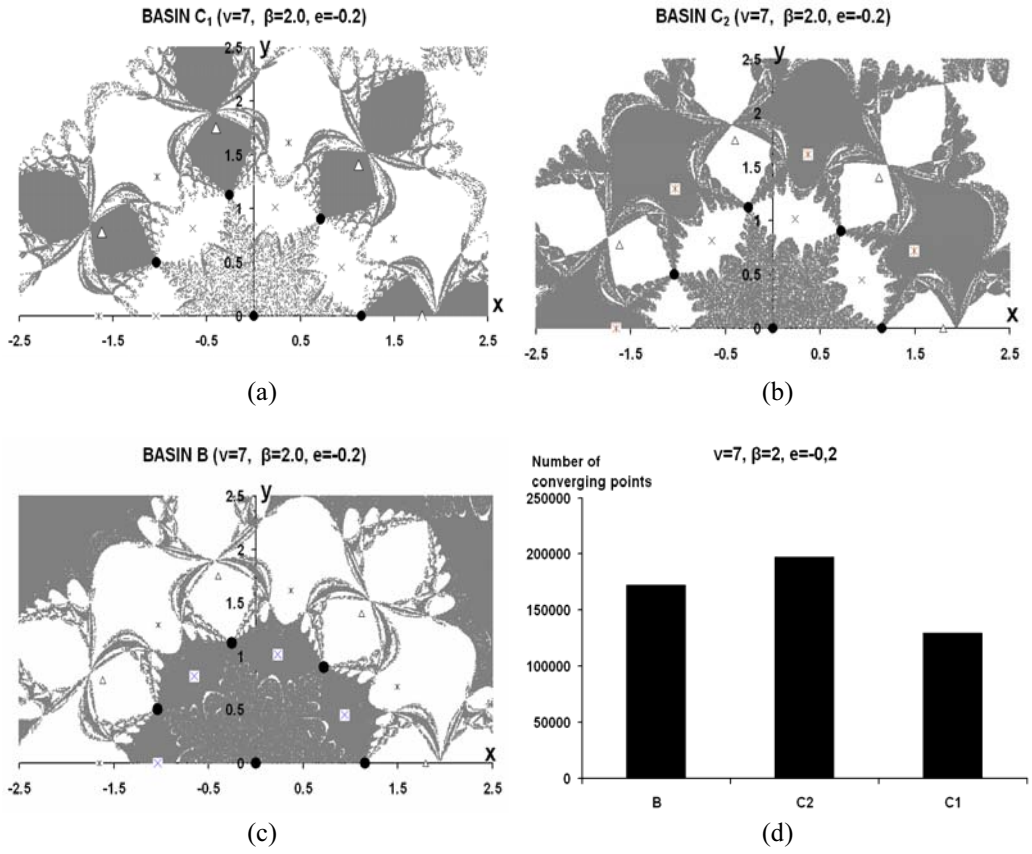

Figure 7. Attracting domains for a configuration with ν=7 and β=2, e=-0.2 (region V of the bifurcation diagram, three equilibrium zones); (a) zone C_1, (b) zone C_2, (c), zone B, (d) bar chart showing the number of the converging points of each equilibrium zone

- The same is true for the rest of the class intervals 11-15 (moderate convergence), 16-20 (slow convergence) and >20 (very slow convergence) steps, which merely consist of dispersed points lying either on the boundaries of the "compact" regions of the previously mentioned class interval, or between the "compact" regions of the other equilibrium zones and they have similar shapes. Naturally, a decreasing density is observed as the number of the steps increases. Since the forms and the development of the subgroups above are similar to the ones of class interval 6-10, we do not think that a further presentation of figures referring to them is necessary.

The bar charts of Figure 8 show the number of the converging points per class interval for each equilibrium zone in the two considered cases with ν=7, β=2, e=-0.1 (Figure 8a) and ν=7, β=2 and e=-0.2 (Figure 8b) respectively. As we can see the class interval 6-10 steps is the largest one.

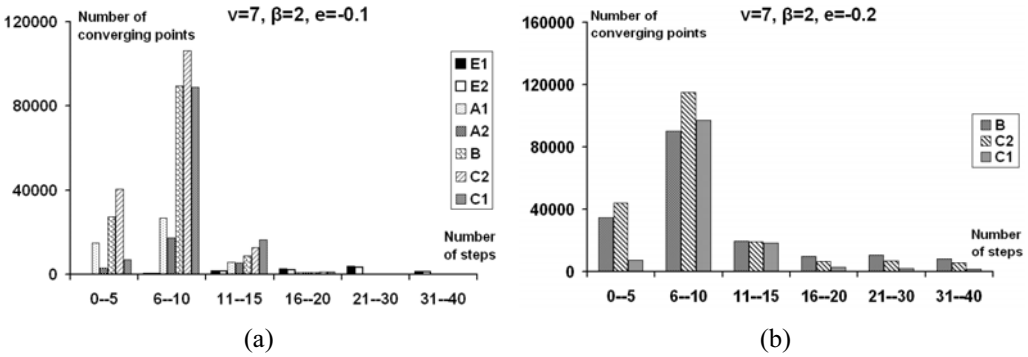

Figure 8. ν=7, β=2. Number of converging points per class interval for each equilibrium zone; (a) e=-0.1, (b) e=-0.2

7. Conclusions and remarks

In the above paper, we have studied the creation, evolution and parametric dependence of the attracting domains in a ring-type N-body model where the central body creates a Manev-type potential. As we have seen, an attracting area is formed for each equilibrium zone. This area consists of a "compact" part and of dispersed points. These points are distributed in the boundaries of the compact parts of the same or of other equilibrium zones. For a particular ν, the evolution of these domains is influenced by both parameters, mass parameter β and Manev's parameter e. Regarding parameter e, when it is positive we observe an evolution which is very similar to that of the pure gravitational case (e=0). However, when e<0 major differences are observed. Two new equilibrium zones, that is E_1 and E_2 may appear and the number of the existing zones may change from seven to five and then to three according to the values of e and β. In all cases, the attracting regions of zones E_1 and E_2 are the smallest, while that of zone C_2 is the greatest. As regards the class intervals of the attracting domains of the equilibrium zones, we must note that the areas corresponding to very fast convergence (within 1-5 steps) consist of the central "compact" parts of the attracting domains of the specific zone that surround the equilibrium positions of this zone and few dispersed points that frame these areas, but also appear near other equilibrium zones. We also found that in all cases the class interval 6-10 steps is the densest.

References

Arribas, M., Elipe, A., 2004. *Bifurcations and equilibria in the extended N-body problem.* Mech. Res. Comm. 31: 1-8.

Elipe, A., Arribas, M., Kalvouridis, T.J., 2007. *Periodic solutions and their parametric evolution in the planar case of the (n+ 1) ring problem with oblateness.* Journal of Guidance, Control and Dynamics, 30: 1640-1648.

Croustalloudi, M., Kalvouridis T. J., 2004. *On the structure and evolution of the 'Basins of Attraction' in Ring-Type N- Body Formation*. In "Order and Chaos in Stellar and Planetary Systems" G. Byrd, K. Kholshevnikov, A. Myllari, I. Nikiforov and V. Orlov, (eds), ASP Conference Series, 316: 93-96.

Croustalloudi M., Kalvouridis T., 2007. *Attracting Domains in Ring-Type N-Body Formations*. Planetary and Space Sci., 55: 53-69.

Haranas, I., Ragos, O., Mioc, V.: 2011. Yukawa-type potential effects in the anomalistic period of celestial bodies. Astrophys.Space Sci., 332 : 107-113

Kalvouridis, T.J., 1999. *A planar case of the n+1 body problem.The 'ring' problem*. Astrophys. Sp.Sci., 260: 309-325.

Kalvouridis, T.J., 2009. *Chaotic and deterministic regions of convergence in the photo-gravitational regular polygon problem of (N+1) bodies.* In Demos Tsahalis (ed.), Proceedings of the 3rd International Conference on Experiments/Process/ System modeling/ Simulation/ Optimization, Athens, Greece, vol I, pp. 135-142.

Maneff, G., 1924. La gravitation et le principe de l' action et de la reaction. C.R. Acad. Sci. Paris, 178: 2159-2161.

Maneff, G., 1930. *La gravitation et l' energie au zero.* C.R. Acad. Sci. Paris, 190: 1374-1377.

Scheeres, D.: 1992. *On symmetric central configurations with application to satellite motion about rings.* Thesis. The University of Michigan, 256 pp.